Published in final edited form as:
J Cataract Refract Surg. 2007 June ; 33(6): 1051–1064.

Photorefractive keratectomy in the cat eye: biological and optical outcomes

Lana J. Nagy, B.S., **Scott MacRae, M.D.**, **Geunyoung Yoon, Ph.D.**, **Matthew Wyble, B.S.**, **Jianhua Wang, Ph.D.**, **Ian Cox, Ph.D.**, and **Krystel R. Huxlin, Ph.D.**
From the Department of Ophthalmology (Nagy, MacRae, Yoon, Wyble, Wang, Huxlin), University of Rochester, Rochester, New York, Bausch & Lomb (Cox), Rochester, New York, USA.

Abstract

PURPOSE— To quantify optical and biomechanical properties of the feline cornea before and after photorefractive keratectomy (PRK) and assess the relative contribution of different biological factors to refractive outcome.

SETTING— Dept. Ophthalmology, University of Rochester, Rochester, New York, U.S.A.

METHODS— Adult cats underwent 6D myopic or 4D hyperopic PRK over 6 or 8mm optical zones (OZ). Pre- and post-operative wavefront aberrations were measured, along with intraocular pressure, corneal hysteresis (CH), corneal resistance factor (CRF), axial length, corneal thickness and radii of curvature. Finally, post-mortem imunohistochemistry for Vimentin and α-smooth muscle actin was performed.

RESULTS— PRK changed ocular defocus, increased higher order aberrations and induced myofibroblast differentiation in cats. However, the intended defocus corrections were only achieved with 8mm OZs. Long-term flattening of the epithelial and stromal surfaces was noted following myopic, but nor hyperopic PRKs. Feline intraocular pressure was unaltered by PRK, but CH and CRF decreased. Over the ensuing 6 months, ocular aberrations and intraocular pressure remained stable, while central corneal thickness, CH and CRF increased back towards normal levels.

CONCLUSIONS— Cat corneas exhibited optical, histological and biomechanical reactions to PRK that resembled those previously described in humans, especially when optical zone size was normalized to total corneal area. However, cats exhibited significant stromal regeneration, causing a return to pre-operative corneal thickness, CH and CRF without significant regression of optical changes induced by the surgery. Thus, the principal effects of laser refractive surgery on ocular wavefront aberrations can be achieved in spite of clear, inter-species differences in corneal biology.

INTRODUCTION

Laser refractive surgery, a method that uses laser energy to ablate and reshape the corneal surface, has become an established form of vision correction. While relatively successful at

Address for Correspondence: Krystel Huxlin, Department of Ophthalmology, Box 314, University of Rochester Medical Center, 601 Elmwood Ave, Rochester, NY 14642, USA, Ph (585) 275-5495, email: huxlin@cvs.rochester.edu

Drs. MacRae, Wang and Yoon have served as consultants to Bausch & Lomb. Dr. Cox is a full-time employee of Bausch & Lomb. The University of Rochester has a research contract with Bausch & Lomb and has licensed intellectual property to them. No other author has a financial interest in any product mentioned.

Cat and human corneas have similar optical reactions to laser refractive surgery despite significant differences in corneal rigidity and regenerative capacity.

treating defocus and astigmatism, negative optical outcomes still occur, including under- and over-correction, regression and increases in the magnitude of higher order optical aberrations (HOA)[1]. While the causes of such problems are clearly multi-factorial, the biomechanical reaction of the cornea to the surgery is considered to be one of the major contributors to negative optical outcomes[2–5]. In turn, corneal biomechanics are affected by a variety of biological parameters such as corneal thickness, area, structural organization, molecular composition, rigidity, as well as by intraocular pressure[2–5]. Most research into the effects of refractive surgery on ocular optics is performed in humans. This provides invaluable data, but is often limited ethically and practically by the needs of the patients. In turn, this limits our ability to properly assess the breadth and complexity of this surgery's effects on ocular optics and especially, biology. Animal models such as rabbits, rodents, cats and monkeys, which are traditionally used to study the biological consequences of laser refractive surgery have taught us much about the wound healing response of the cornea[6–10]. However, it has been difficult to correlate these biological changes with surgically induced changes in ocular optics. This is due partly to the fact that most measures of ocular optical quality require steady fixation and most animal models are not able to provide that[11–14]. On the other hand, when anesthetized animals are used, there are significant alterations in tear film quantity and quality, which negatively affect optical quality[15].

We have developed a unique animal model in which the problem of acquiring reliable measures of optical quality has been overcome. Using established psychophysical methods[16–19], normal, adult cats are trained to repeatedly and precisely fixate small visual targets on a computer screen, while a compact Shack-Hartmann wavefront sensor is aligned to the line of sight and the pupil center of each eye, as is done when measuring ocular wave aberrations in humans[20]. This allows for accurate, reproducible measurements of ocular wave aberrations at multiple time-points before and after laser refractive surgery, in the awake, fixating, normally-blinking state. Using this paradigm, we recently demonstrated that the optical quality of the un-operated, adult cat eye is as good as that of the normal, adult human eye[20]. Aside from its excellent optical quality, several other factors make the cat eye an excellent model for refractive surgery research. Cat corneas are by no means identical to human corneas. For instance, they have greater diameters than human corneas[21–25]. However, some of the cat corneal parameters most likely to affect corneal biomechanical properties (thickness, cellular and structural organization, molecular composition) closely approximate those of the human cornea[25–31]. This is a critical point because the cornea is the ocular structure contributing to the majority of the power of the eye[32] and to the majority of higher order optical aberrations induced after laser refractive surgery[33, 34]. While rabbits are often the animal model of choice in refractive surgery research, cats have also been used successfully in studies of corneal wound healing following refractive procedures[8, 35, 36]. By adding the ability to reliably quantify optical wave aberrations to the repertoire of experimental manipulations that can be performed in cats, we are now in a stronger position to be able to correlate optical, biomechanical and biological outcomes of ophthalmologic interventions in a single animal model. Such studies are critical if we are to understand the biological and biomechanical substrates of negative optical outcomes following manipulations of the ocular surface.

The specific goals of the present study were to use the awake-fixating cat animal model to (1) quantify optical and bio-mechanical properties of intact cat corneas, (2) assess the effect of photorefractive keratectomy (PRK), a form of laser refractive surgery, on the optical, biological and biomechanical properties of cat corneas in situ, and (3) assess the relative contribution of different biomechanical factors, in particular corneal area and native corneal rigidity, for attaining optimal refractive outcome following PRK.

METHODS

Subjects

Data were obtained from 26 eyes of 14 normal, male, domestic short hair cats (*felis cattus*). Two eyes from one animal were eliminated from our analysis because of post-operative complications (persistent inflammation and development of corneal sequestra). All cat procedures were conducted in accordance with the guidelines of the University of Rochester Committee on Animal Research, the ARVO Statement for the Use of Animals in Ophthalmic and Vision Research, and the NIH Guide for the Care and Use of Laboratory Animals. We measured corneal visco-elastic properties and intraocular pressure in 16 eyes from 8 young, adult human subjects, none of whom had undergone refractive surgery or exhibited ocular pathologies. Axial lengths were also measured in 12 eyes from 6 of these subjects. All human measurements (axial length, hysteresis, CRF and intraocular pressure) were conducted after the administration of informed consent and in strict adherence to the tenets of the Declaration of Helsinki.

Ocular wave aberrations in awake-fixating cats

Cats were trained using standard psychophysical methods[16, 20]. Briefly, each cat was placed inside a magnetic field driven by 50cm coils and its head was immobilized using an implanted cranial post. Electrical signals from an implanted, subconjunctival eye coil were captured and calibrated using an eye coil phase detector (Riverbend Electronics, USA). The animals were trained to fixate small (0.03^{o} visual angle) spots of light on a dark, 19” ViewSonic PF790 computer monitor placed 48cm from their eyes. They were rewarded for maintaining their gaze within an electronically defined, 1°square window around each fixation spot and trained until they could maintain steady fixation within this window for 2.5-5s. A compact Shack-Hartmann wavefront sensor was placed on a height-adjustable platform between the cat and the computer monitor[20]. An infrared pupil camera was used to align the wavefront sensor to the pupil center of one eye, while the other eye fixated a spot on the computer monitor[20]. Spot array patterns were collected pre-operatively and 1, 3 and 6 months following PRK. Wave aberrations were calculated from these spot arrays using the Zernike polynomial expansion up to the 10th order. Only data pertaining to the 2nd-5th orders (j=3–20) are presented here since they are most significant for visual performance. The amplitude (μm) of individual Zernike terms was calculated for the largest pupil diameter that could be obtained (usually 8–9mm) and MatLab (MathWorks, USA) was used to derive their corresponding amplitude for a 6mm diameter aperture, in agreement with OSA standards[37]. The accuracy of this renormalization of the Zernike coefficients was verified by analyzing spot array patterns over a 6mm pupil aperture and comparing the aberrations measured with those calculated by interpolation from a 9mm aperture. There was no significant difference between these two methods for any of the Zernike coefficient values up to j=20. The magnitude of the defocus terms (Z_2^0, j=4) was converted to Diopters using the formula:

$$\text{Diopter (D)} = \frac{-4\sqrt{3}Z_2^0}{(r)^2}$$

where r=radius (mm) of the analysis pupil

The total root mean square (RMS) of j=3–20, and the higher order RMS (HORMS) for j=6–20 were also calculated as described previously[20].

Corneal thickness and radii of curvature

Optical coherence tomography (OCT) was used to image the cornea across the nasal temporal meridian both before and 1, 3 and 6 months after PRK in the four cat eyes that underwent

ablations over 8mm OZs. This provided two eyes with hyperopic and two eyes with myopic corrections. To undergo OCT imaging, the animals were first anesthetized with a mixture of Ketamine and Xylazine (5mg/kg and 1mg/kg respectively) and a drop of Genteal Eye Gel (CibaVision, USA) was administered to each eye. The anesthetized cats were placed in a custom-made head-restraint device in order to hold their head stable for imaging. Our custom-made, anterior segment OCT[38, 39] was aligned to the apex of each cornea. Using a 1310nm scanning laser, the OCT recorded a video-stream of the cornea at a rate of eight frames per second, as previously reported[38, 39]. A mean, normalized profile of backscatter light intensity over the central 105μm of each cornea was generated from twenty-five corneal images isolated from the video stream. In each intensity profile, a peak or maximum amplitude of light reflectivity, corresponding to an interface between two different layers, was used to obtain the epithelial, stromal and total corneal thicknesses[38, 39]. These same OCT images were also used to calculate corneal surface curvatures. Following scaling to correct for optical distortion of each image, a custom, edge-detection algorithm was used to select pixels within a user-defined zone that encompassed either the epithelial-tear film (plus gel) interface, the epithelial-stromal interface or the stromal-endothelial interface. The software then fitted a best-fit sphere to each interface and determined its radius of curvature over the central 6mm of the cornea (for epithelial and stromal surfaces) and the central 5mm of cornea (for the endothelial surface). PRK-induced changes in these three radii of curvature were then calculated and their absolute values were computed at 1, 3 and 6 months after PRK.

Intra-operative ultrasonic pachymetry was performed to obtain an estimate of the amount of stromal tissue removed during PRK. Five to 10 readings were collected at the center and the inner edge of a 6 or 8mm marking ring using a Corneo-Gage Plus2 Ultrasonic Pachymeter (Sonogage, USA) immediately before and immediately after PRK over 6 or 8mm OZs respectively. Central thickness measurements were important in assessing how much tissue had been removed in myopic PRKs, where most of the tissue removal occurs in the center of the ablation. However, in hyperopic PRKs, most of the tissue removed is at the ablation periphery – it is at this “trough” that peripheral measurements of corneal thickness were carried out with the ultrasonic pachymeter. Importantly, pre-operative values of total, central corneal thickness collected with the Sonogage Pachymeter in our cats were not significantly different from those obtained with the OCT in the same animals (data not shown).

Ocular axial length

To exclude the possibility that small refractive changes observed after PRK in cats might be due to an aggressive emmetropization process, partial coherence interferometry with the IOLMaster (Zeiss, Germany) was used to measure ocular axial length pre-operatively, 1 and 3 months after PRK. The cats were anesthetized and positioned in a head-holding device with their head facing forward. The nictitating membranes were retracted with 2.5% Phenylephrine Hydrochloride drops (Bausch & Lomb, USA) and the eyes were blinked manually to preserve surface quality. The IOLMaster was aligned according to standard procedures and 5 measurements were collected per eye. Similar measurements were carried out in 12 eyes of 6 human subjects, whose heads were stabilized using a chin/forehead rest. They were asked to fixate the instrument's red target light while 5 measurements were collected from each eye.

Measurements of intraocular pressure, corneal hysteresis and corneal resistance factor

For cats, these measurements were collected in the anesthetized state. Genteal Eye Gel (CibaVision, USA) was used to preserve corneal hydration. The Ocular Response Analyzer - ORA (Reichert, USA) - was automatically aligned to the center of each eye and 5-6 measurements of corneal hysteresis (CH), Corneal Resistance Factor (CRF), Goldmann-like Intraocular Pressure (IOPg) and Cornea-Compensated Intraocular Pressure (IOPcc) were collected[2, 40]. For human measurements, the subjects first applied a drop of Genteal Gel to

each eye in order to replicate conditions for data collection in the cats. They sat with their heads resting in the machine's chin/forehead rest and were asked to fixate the instrument's green target, while 5–6 measurements were collected from each eye.

Our experimental setup provided an excellent opportunity to assess the repeatability of measures collected using the ORA in a cat animal model, comparing it with repeatability of the same instrument in human subjects. To this effect, we computed the coefficients of variation (COV) for measurements of CH, CRF, IOPg and IOPcc in our sample of cats (pre-operatively) and normal human eyes. In all cases, COV was calculated by dividing the standard deviation of the mean obtained from each measurement session (consisting of 5-6 measurements) by the mean value obtained during that session. The COV was then expressed as a percentage of the mean for each measurement type and session. The lower the COV, the more repeatable the measurements obtained with the ORA.

PRK

Five cat eyes underwent 6D myopic PRK, three over 6mm optical zones (OZs) and two over 8mm OZs, with OZ defined as a "true" optical zone, not including the transition zone that was present in every ablation type. Another five eyes underwent 4D hyperopic PRK, three over 6mm OZs, and two over 8mm OZs. All procedures were conventional, spherical ablations with transition zones. They were performed under surgical anesthesia, using a Technolas 217 laser (Bausch & Lomb, USA). Pre-operatively, the corneas were treated with 0.5% Proparacaine Hydrochloride (Bausch & Lomb, USA) and the nictitating membrane was retracted with 2.5% Phenylephrine Hydrochloride (Bausch & Lomb, USA). The eyes were stabilized using temporary sutures placed on the inferior and superior portions of the conjunctiva and attached using a 2-inch mosquito clamp to the cheek skin or brow. Before the actual ablation, each eye was marked with a blue 6 or 8mm ring centered on the dilated pupil. Pachymetry was performed as described above. The epithelium was then scraped off and measurements of stromal thickness were performed as described earlier. The difference between the pre- and post-scrape pachymetry yielded the approximate central epithelial thickness of each cat eye. Following surgery, ultrasonic pachymetry was repeated to estimate the amount of tissue removed by the ablation. The cornea was not irrigated after removal of the epithelium in order to minimize swelling that would result from such hydration. After surgery, the cats received 2 drops of TobraDex (Alcon, USA) per eye, which was continued once per day until the surface epithelium healed (~ 1 week post-operatively).

Post-mortem histology

Six cats underwent 6D myopic PRK over 6mm OZ for the purpose of obtaining post-mortem histopathology. Three cats were sacrificed 1 month post-operatively and another three cats were sacrificed 3 months after PRK. For euthanasia, cats were anesthetized with a mixture of Ketamine and Xylazine (5mg/kg and 1mg/kg respectively) before receiving an overdose of Sodium Pentobarbital (100 mg/kg). Once all reflexes had disappeared, the corneas were excised and drop-fixed in a solution of 1% Paraformaldehyde in 0.1M phosphate buffered saline (PBS), pH 7.4 for 10mins, after which they were transferred to a solution of 30% sucrose in 0.1M PBS, and stored at 4°C for 2 days. Once suitably cryo-protected, the corneas were embedded in Tissue Tek® O.C.T. Compound (Sakura Finetek, USA) and serial, sagittal sections were cut on a cryostat at 20μm thickness. The sections were collected on microscope slides and stored in a –20°C freezer until ready to stain.

A set of sections from each cornea was stained with Hematoxylin according to routine protocols. Adjacent sets were stained with antibodies against Vimentin to label corneal keratocytes or α-smooth muscle actin (αSMA) to label myofibroblasts. The immunoreactions were performed in a humidified chamber at room temperature. Sections were first incubated

with primary antibodies – monoclonal mouse anti-Vimentin (Clone V9, Sigma, USA – used at 1:100) or monoclonal mouse anti-αSMA (Sigma, USA – used at 1:50) – overnight. They were rinsed with 0.1M PBS and incubated for 4 hours with biotinylated secondary antibodies (Vectastain ABC Elite Kit, Vector Labs, USA). After further rinsing, the sections were incubated with ABC reagent (Vectastain ABC Elite Kit, Vector Labs, USA) for 1 hour. After another set of rinses, they were incubated with 0.5% diaminobenzidine (DAB, Sigma, USA) in 0.1M PBS in the presence of hydrogen peroxide to generate a permanent, brown product. After a final set of rinses, the sections were dehydrated, cover-slipped and examined using an Olympus AX70 microscope. All photomicrographs presented in the results section were collected via a high resolution-high sensitivity video camera interfaced with a PC running the ImagePro software (MediaCybernetics, USA). ImagePro was used to capture images, which were then transferred to Microsoft Powerpoint for assembly and labeling.

Statistical analysis

Mean values for different groups were compared using the two-tailed, unpaired Student's t-test. Values of $P<0.05$ were considered statistically significant. Changes in defocus, HORMS and corneal radii of curvature induced by myopic or hyperopic PRK over 6 or 8mm OZs, between 1 and 6 months post-op were tested with a mixed-factorial analysis of variance (ANOVA), with group (i.e. 6 versus 8 mm OZs or myopic versus hyperopic PRKs) as between-subject factors, and post-operative time as the repeated measure. In all cases, a P value<0.05 was considered significant.

RESULTS

Pre-operative ocular biometry

Table 1 compares cat biometric values measured in this study with human biometric values, some measured presently, others collected from the literature. This comparison revealed some similarities and several significant differences between cat and human corneas. Cat and human IOPcc were not significantly different from one another. In addition total and epithelial thicknesses of the central cat cornea were within the normal range reported for humans. However, axial length, corneal hysteresis, IOPg and CRF were all significantly smaller in cats than in humans (two-tailed Student's t-test, $P<0.05$).

Our calculation based on measurements collected with the Reichert ORA in cats and humans revealed that COVs for CH, CRF and IOPg were significantly smaller in humans than in cats. CH COV was 7.9±5% in humans and 16.3±9% in cats ($P<0.05$, two-tailed Student's t-test). The COV for CRF measurements was 6.8±4.9% in humans and 18.4±9.4% in cats, while the COV for IOPg measurements was 7.5±3.5% in humans and 12.0±5.4% in cats (both $P<0.05$, two-tailed Student's t-test). However, the COV for IOPcc measurements was not statistically different between the two species (12.6±8.2% for cats and 14.0±8.2% for humans; $P>0.05$, two-tailed Student's t-test). However, in all cases when a significant difference was observed between mean values of ORA measurements collected in cats and humans (IOPg, CH and CRF), this difference (28% for IOPg, 41% for CH and 61% for CRF) was significantly larger than the COVs for that measurement in either species.

Pre-operative optical aberrations

Our sample of pre-operative cat eyes exhibited excellent optical quality. The magnitude of lower and higher order wavefront aberrations was small (Figure 1C and D), with total RMS averaging 1.27±0.66μm. HORMS was 0.41±0.24μm, representing 10.3% of the variance of total RMS.

Effect of PRK on optical aberrations

6 mm OZ—Laser refractive surgery over 6mm OZs in cats induced significant hyperopic (following myopic PRK) and myopic (following hyperopic PRK) shifts in their defocus term (j=4) relative to pre-operative values (Figure 2). However, one month after surgery, only 2.2 ±0.4D and –0.8±1.2D of defocus change were observed after -6D myopic and +4D hyperopic ablations, respectively (Figure 4A). The amount of astigmatism (j=3 and 5) induced was relatively small in all cases (Figure 2) but higher order aberrations increased significantly (Figure 3). When grouping myopic and hyperopic ablations one month post-operatively, HORMS increased by 0.78±0.51μm relative to pre-operative values (two-tailed Student's t-test, $P<0.05$), representing ~32% of the variance of total RMS. Most of this increase was due to 3rd order aberrations, especially vertical coma (j=7), which increased by 0.29±0.82μm relative to pre-operative values (Figure 3). Spherical aberration (j=12) became more positive by 0.18±0.20μm following myopic treatments and more negative by 0.47±0.61μm following hyperopic treatments (Figure 3). An analysis of variance revealed that between one and six months after PRK over a 6mm OZ, cats showed no significant changes in defocus (P=0.206 for myopic PRK; P=0.06 for hyperopic PRK – Figure 4A) or HORMS (P=0.678 for myopic PRK; P=0.257 for hyperopic PRK - Figure 4B).

8 mm OZ—One month after PRK over an 8mm OZ, cats experienced a 4.5±1.2D hyperopic shift (following 6D myopic PRK – Figures 2, 4) and a –4.2±1.6D myopic shift (following 4D hyperopic PRK – Figures 2, 4), which showed no statistically significant changes over the ensuing 5 months (P=0.206 for myopic and P=0.06 for hyperopic PRK, ANOVA - Figure 4A). However the same ANOVA revealed a significant effect of OZ size on defocus change after myopic PRK, which resulted in consistently greater changes in defocus from pre-operative levels in 8mm compared to 6mm OZs (P=0.028). The ANOVA revealed this to be true at all time-points examined. For hyperopic PRK, ANOVA revealed no significant effect of OZ size, but a significant interaction between OZ size and post-operative time (P=0.048), which suggests the existence of slightly different temporal trends for 4D hyperopic ablations over 6 versus 8mm OZs. Indeed, inspection of Figure 4A does illustrate the greater temporal variability in the defocus term for 4D hyperopic ablations over 8mm compared to the same ablations performed over 6mm OZs.

HORMS induced by PRK over 8mm OZs exhibited no main effect of OZ size over the 6 months following the surgery (P=0.580 for myopic PRK; P=0.306 for hyperopic PRK, ANOVA) and no significant interaction between OZ size and post-operative time (P=0.056 for myopic PRK; P=0.564 for hyperopic PRK, ANOVA). On average, HORMS increased by 0.64±0.36μm relative to pre-operative values, but this represented only ~15% of the total variance of RMS one month after PRK. Most of the increase in HORMS was again due to increases in coma terms (j=7 and 8), while spherical aberration (j=12) changed relatively little (+0.20±0.13μm after myopic and –0.32±0.08μm after hyperopic PRK - Figure 3). Overall, HORMS did not change significantly from 1 to 6 months postoperatively (P=0.444 for myopic PRK; P=0.257 for hyperopic PRK, ANOVA - Figure 4B), although we cannot exclude the fact that this lack of significance may be due to our small sample size.

Effect of PRK on ocular biometry

PRK removed similar amounts of corneal stroma in cats as predicted by the Technolas laser algorithm (Bausch & Lomb, Inc.), which is based on the instrument's performance in humans. For cat ablations over 6mm OZs, the laser removed 72±28μm of stromal tissue, as assessed from intra-operative pachymetry. As indicated earlier, this value was computed from pachymetry measurements collected at the deepest parts of the myopic and hyperopic ablations - centrally for myopic ablations and just inside the ablation zone for hyperopic ablations. The amount of tissue actually removed by the 6mm ablations in cats was not significantly different

(P=0.1, two-tailed Student's t-test) from the depth of removal (91±14μm) predicted for these ablations by the Technolas 217Z laser's technical documentation (Bausch & Lomb, Inc.). However, the 8mm optical zone ablations yielded significantly less tissue removal than was predicted by the laser algorithm - only 110±22μm of stromal tissue was removed compared to the predicted 172±20μm (P<0.05, two-tailed Student' t-test).

Since only corneas that received PRK over 8mm OZs attained close to intended refractive corrections, they were selected for OCT imaging to examine the rate of remodeling of the different corneal layers (i.e. epithelium versus stroma) and changes in the curvature of the epithelial, stromal and endothelial surfaces. OCT measurements of the four cat corneas that underwent myopic (N=2) and hyperopic (N=2) ablations over 8mm OZs (Figure 5A and B) revealed that as expected, significantly more stromal tissue had been removed from the central cornea in myopic treatments than in hyperopic treatments. By 1 month after myopic PRK, stromal, epithelial and hence, total thickness of the central cornea had returned to normal levels, remaining stable over the ensuing 5 months (Figure 5A). Cats that underwent hyperopic treatments also exhibited a return to normal central stromal and epithelial thicknesses, but this return appeared to be more gradual than after myopic PRK, with changes still occurring 6 months after PRK (Figure 5B).

One month after 8mm myopic PRK, the radius of curvature of the central 6mm of the epithelial surface increased from 8.96±0.9 mm pre-operatively to 9.74±0.03 mm (Figure 6B). The radius of curvature of the stromal-epithelial interface (labeled "stromal" in the figures) also increased from 8.9±0.8 mm to 9.9±0.1 mm (Figure 6B). By contrast, the endothelial radius of curvature changed less (8.1±0.4 mm pre-op to 8.5±0.1 mm at 1 month post-op – Figure 6B). The flattening of the two anterior corneal surfaces was maintained over the ensuing 5 months following myopic PRKs. This paralleled the initial hyperopic shift (from pre-op to 1 month post-op) and subsequent refractive stability (from 1-6 months post-op) observed for the defocus term in cats treated with 8mm OZs (Figure 4A). One month after hyperopic PRK over 8mm OZs, a relatively small increase in anterior, stromal and endothelial radii of curvature was observed over the central 6mm of cornea (Figure 6B). These flatter corneas persisted out to three months post-hyperopic PRK, but unlike corneas with myopic treatments, they became steeper than before surgery by the 6th month after hyperopic PRK. An analysis of variance revealed the observed differences in the curvature changes between myopic and hyperopic ablations over time to be most significant at the epithelial surface and the stromal/epithelial interface (P= 0.009 and 0.025 respectively). The effect was not significant at the endothelial surface (P=0.365). The most striking observation, however, is that we saw no decrease in the anterior and stromal radii of curvature over the first 3 months after hyperopic PRK (Figure 6B), even though the myopic shift in the defocus term seen in these cats (Figure 4A) would predict that there should be such a change.

One and 3 months after PRK, the average axial length in the cat eye was 22.8±0.1mm and 22.9 ±0.2mm respectively, which was not significantly different from pre-operative values (two-tailed Student's t-test, P>0.05).

Finally, one month after PRK, whether using myopic or hyperopic treatments (no significant effect of group observed), cat CH decreased significantly from 8.4±1.8mmHg to 4.7 ±0.4mmHg. However, it recovered back to normal levels over the next 5 months (Figure 7A). Similarly, CRF decreased significantly from 7.0±1.5mmHg pre-operatively to 3.1±1.0mmHg 1 month after PRK, increasing slightly over the next 5 months (Figure 7B). By contrast, IOPg and IOPcc were not significantly affected by PRK, although IOPg appeared to exhibit a slight decrease post-operatively relative to pre-operative values (Figures 7C and **D**).

Effect of PRK on cat corneal histology

As shown in Hematoxylin-stained sections (Figure 8), the normal feline cornea possesses histological structure resembling that of other mammalian corneas examined to date. The cat cornea is covered by a stratified epithelium, a stroma populated by keratocytes that normally stain positive for Vimentin but not αSMA, and a single-cell layer endothelium. A thin Bowman's layer separates the epithelium from stromal keratocytes in un-operated corneas, but disappears following PRK (Figure 8). Decemet's membrane is also present, separating the stroma from the endothelium (Figure 8). Following PRK, Hematoxylin staining showed an increased density of stromal cells under the re-generated epithelium, which persisted out to 3 months after surgery (Figure 8). At least some of the stromal cells that lay under the ablation epithelium appeared to be keratocytes, as they stained positive for Vimentin. One month after PRK, a proportion of these stromal cells also stained positive for αSMA (arrowed in Figure 8), suggesting that they were myofibroblasts. However, while the increased density of sub-ablation keratocytes persisted out to 3 months post-operatively, there was a significant reduction in α SMA expression under the ablation epithelium at this time-point (Figure 8).

DISCUSSION

The contribution of corneal biology to the optical changes caused by laser refractive surgery is a topic of great current interest. Significant effort is being directed towards understanding what aspects of corneal biology and biomechanics are responsible for the negative optical outcomes of this procedure. Our goal here was to examine optical changes induced by PRK in a cat animal model. While similar in gross structure and thickness, cat and human corneas differ in surface area, corneal hysteresis (CH), resistance factor (CRF) and regenerative capacity, offering an interesting paradigm to evaluate the relative importance of these factors for refractive outcome. However, what makes cats a particularly good animal model for our studies is that they can be trained to fixate visual targets with the same degree of precision as humans[16]. This enabled us to measure wavefront aberrations in cats under the same conditions (i.e. in the awake-fixating state) as in humans. As a result, we were able to monitor surgically induced changes in ocular wavefront aberrations, corneal thickness, shape and rigidity at the same time points.

Similarities and differences between normal cat and human corneas

Our measurements revealed cat corneas to possess similar total central thickness, thickness of epithelial and stromal layers, and general anatomical organization as human corneas[21, 27, 41–45]. In addition, we found no significant differences between cat and human IOPcc, suggesting that the cat cornea is under similar internal pressures as the human cornea. However, the surface area of cat corneas appeared significantly larger than that of human corneas. To verify this, we used published, average corneal diameters[21–25] to first calculate the sagittal height of the "average" cat and human cornea:

$$H = h(R) - h(0)$$

$$h(R) = \frac{C \times R^2}{1 + \sqrt{1 - (k \times C^2 \times R^2)}}$$

where H is the total height of the cornea, C = curvature of the surface (1/radius of curvature (r)), R = corneal radius, measured from the center of the cornea to the corneo-scleral junction, and k = conic constant, in this case a value of 1, assuming a spherical dome. The surface area of the prototypical cat and human cornea was then computed using the standard formula for the surface area of a spherical dome:

$$SurfaceArea = 2\pi Hr$$

This gave an approximate surface area of ~316 mm^2 for the average feline cornea and ~130 mm^2 for the average human cornea. Thus, cats possess corneas that are about 2.4 times larger than human corneas, something we posit may have significant implications for refractive outcome following laser ablation (see below).

The native biomechanical properties of cat and human corneas also appeared to differ significantly. Both CH and CRF were smaller in cats than in humans pre-operatively, suggesting that the cat cornea is normally less rigid than the human cornea[2, 40]. It is unlikely that this difference was due to measurement error. While coefficients of variation were greater for ORA measurements collected in cats than in humans, these coefficients of variation were always significantly smaller than the differences observed between cat and human data. The greater coefficients of variation in cats are probably due to the fact that unlike humans, cats were not awake and fixating the machine' target when measurements were collected. They were anesthetized and while their eyes were wide open, the experimenter had to estimate ocular alignment to the ORA 5-6 times during each measurement session. A parallax-driven error in ocular alignment is a very likely cause of our large coefficients of variability in cats. Aside from this however, the parametric data obtained in our small sample of human subjects with regards to CH, CRF, intraocular pressure and ocular axial length were consistent with previously published measurements[2, 25, 40, 46]. Since the same instruments (the ORA and IOL Master) were then used in our sample of cats, we are relatively confident that our animal data are comparable with data in the human literature.

Low corneal rigidity, usually seen after laser refractive surgery and in keratoconus[2, 47], is thought to imply biomechanical instability and is often predictive of pathological reactions to laser refractive surgery, including the development of keratectasia[48–50]. Why normal cat corneas should have low hysteresis and CRF remains to be determined. Perhaps the collagen fibril arrangement needed to support the greater surface area of feline corneas differs from that needed to support human corneas. Part of this difference may lie in the manner in which collagen fibrils that cover the cornea integrate with limbal fibers. The specific nature of this arrangement is thought to be important for the maintenance of the different corneal and scleral curvatures[29, 51, 52], and has been postulated to influence corneal rigidity[29, 51, 52]. Alternatively, the proteoglycan-collagen fibril organization, known to affect viscoelastic properties of the cornea[53], may differ in the two species. Yet another possibility is that the thinner feline Bowman's membrane[28] does not stabilize its cornea to the same degree as its thicker counterpart in humans[28].

Effects of PRK on feline corneal biometrics and wound healing

In spite of their native differences in corneal area and rigidity, cat and human eyes exhibited many similarities in their biomechanical and cellular reaction to laser refractive surgery. "True" postoperative IOP in the cat, perhaps best represented by IOPcc[40], was unchanged by refractive surgery, just as it has been reported in humans[40, 54]. On the other hand, PRK significantly decreased corneal rigidity (CH and CRF) in the cat, a phenomenon also reported in humans following laser refractive surgery[40, 47]. However, feline CH and CRF slowly increased between 1 and 6 months post-PRK, paralleling a gradual increase in stromal and total corneal thickness. This supports the notion that corneal rigidity is strongly influenced by wound healing and the changes in stromal and total corneal thickness[40] that accompany this process. It also illustrates the strong regenerative capacity of the cat cornea following injury, consistent with a recent report by Acosta and colleagues[55] who reported strong corneal regeneration following implantation of supradescemetic keratoprostheses in cats. Corneal regrowth has also been reported in rabbits[56] but occurs to a much lesser extent in humans after PRK[57]. Indeed, corneal remodeling in the cat brought total central corneal thickness back to pre-operative values by the 6^{th} month after PRKs that removed, on average, almost 100μm of central stroma. For cats

with myopic PRK, most of the re-thickening occurred within the first post-operative month, with slower re-growth taking place between 1 and 6 months post-PRK. For cats with hyperopic ablations, the central stromal re-thickening was a lot slower (and of a lesser magnitude) than in cats with myopic ablations, but the final outcome was also a return to pre-operative stromal and epithelial thicknesses by the end of the 6th post-operative month. As previously reported for both humans and rabbits after PRK[56–58], most of the observed corneal re-growth affected the stroma, while epithelial thickness, which returned to its pre-operative levels by one month post-PRK, remained stable thereafter. While a detailed examination of the cellular wound healing response to PRK in the cat was beyond the scope of this study, we did ascertain that the cat cornea's cellular reaction to PRK was largely similar to that reported previously in this species[8], as well as in rabbits[7], monkeys[59] and humans[60–62]. The stratified epithelium re-formed over the ablation zone without reforming Bowman's layer. αSMA-positive myofibroblasts appeared and occupied the sub-epithelial zone under the ablation. αSMA reactivity was maximal at around 1 month after PRK, decreasing afterwards, but the sub-ablation stroma remained hypercellular, at least out to 3 months after surgery.

Effects of PRK on feline ocular optics

In terms of optical reaction to refractive surgery, defocus changed in the intended direction after PRK in cats, becoming more myopic after hyperopic treatments and more hyperopic after myopic treatments. Cats also exhibited an increase in the magnitude of higher order aberrations up to and including the 5th order Zernike terms. Changes in the amount and sign of spherical aberration were within the range reported after equivalent PRK in humans[63, 64]. Cats also exhibited relatively large increases in coma-type aberrations, probably because the animals were anesthetized for surgery and Phenylephrine drops were used to keep their nictitating membranes retracted. These drops dilated their pupils beyond 12 mm in diameter, making centration of the laser ablation on the pupil very difficult[65], a phenomenon that is known to increase coma[66].

One notable difference between optical outcomes in cats and humans undergoing comparable refractive ablations over a 6mm OZ was that cats achieved very little (37% and 20% respectively) of the intended myopic and hyperopic refractive changes. Since cat axial lengths did not change significantly after PRK, rapid post-operative emmetropization was unlikely to be responsible for these severe under-corrections. The IOL Master used in the present study can measure axial lengths ranging from 14 to 40mm with a resolution of ±0.01mm. Reproducibility of the device is excellent, with a standard deviation of ±0.03mm in human eyes. Taking 1/*f*, where *f* is the axial (focal) length of the eye, ~0.5mm of axial length change would be needed to induce 1D of power change in the cat eye. This was larger than the standard deviation of our axial length measures and was never observed.

One factor known to significantly benefit refractive outcome is a larger optical zone[67, 68]. Given the larger area of cat versus human corneas, we hypothesized that our under-corrections with 6mm OZs could be due to the proportionately smaller surface area that this optical zone covers in the cat eye. Indeed, a 6mm OZ ablates ~20% of the average human corneal surface area, but only 9% of the average cat corneal area. Increasing cat OZs to 8mm (~20% of the cat's total corneal surface area) achieved 75% and 105% of our intended myopic and hyperopic corrections, respectively. The amount of higher order aberrations induced by 8mm OZs relative to the total amount of monochromatic aberrations was also smaller than for 6mm OZs. That a larger OZ should be advantageous for refractive outcome, has previously been reported in humans[69–72] and may be due to a combination of factors that involve a different biomechanical reaction of the cornea to a larger, deeper cut, as well as to differences in the wound healing response.

Finally, consistent with the long-term stability previously reported for comparable refractive ablations (i.e. 6D myopic or 4D hyperopic PRK over 6mm OZs) performed in humans[73, 74], no significant regression of the achieved defocus or HORMS change was observed between 1 and 6 months post-PRK in the cat, although both defocus and HORMS appeared more variable following hyperopic than myopic ablations. Interestingly, the relative post-PRK refractive stability in the cat occurred in the presence of significant post-operative central stromal and epithelial remodeling, which, as mentioned earlier, returned central corneal thickness back to normal levels by the 6th month post-PRK. When stromal remodeling was reported in rabbits after PRK[56], it was always assumed (althouth not proven) to accompany or cause refractive regression. This is because in humans, the relatively small amount of stromal thickening (~8%/year) that occurs after PRK is well-correlated with refractive regression[57]. Our findings in cats with PRK suggest that the phenomena of stromal thickening in cats/rabbits and humans may in fact be very different. Indeed, one should probably not assume regression of optical refraction just because central corneal thickness returns to normal after surgery, especially in species that exhibit an aggressive stromal wound healing reaction. Perhaps in cats, the corneal re-growth occurs in such a way as to preserve the new surface profile imparted by the laser ablation. In fact, our observation that anterior (epithelial surface and stromal/epithelial interface) radii of curvature increased and then remained stable in cats between 1 and 6 months after myopic PRK supports this hypothesis. What is not so easy to reconcile is our observation of a slight increase in anterior corneal radii of curvature following hyperopic PRK in the cat at the 1st and 3rd months post-op, in spite of a significant myopic shift in the defocus term at the same time-points. One potential explanation for this contradictory result is our use of best-fit spheres to estimate the radii of curvature of the markedly non-spherical epithelial and stromal surfaces after hyperopic PRK. Further refinement of our surface-fitting algorithm will be necessary to resolve this issue.

Conclusions

The present study describes results from a cat animal model of human PRK in which it is possible to carry our measures of corneal biology, biomechanics and optical quality at the same time-points. Using this model, we highlighted a particularly important role of ablation optical zone *relative* to the total corneal area for attaining a given refractive change in corneas with natively low hysteresis and CRF. In addition, we showed that stromal and epithelial remodeling are not necessarily associated with refractive regression in the cat, a species which like the rabbit, exhibits aggressive wound healing following laser refractive surgery. The native differences in corneal properties and wound healing that exist between cats and humans are revealing a rather more complex relationship between corneal biology, biomechanics and ocular optics than previously envisaged. Defining and understanding this relationship should help us develop more effective therapeutic manipulations to optimize the optical outcomes of corneal surgeries in humans.

Acknowledgements

The authors wish to acknowledge the excellent technical work of Margaret Beha in behavioral training and testing of the cats and for carrying out the feline ORA measurements. We thank John Swanstone for his programming expertise and Tracy Bubel for histological processing of the cat corneal tissue and for Hematoxylin staining. We thank Emily Brandon, Shawn Kenner and Sally Jensen for their analysis of spot array patterns, Terry Schaeffer for carrying out the IOLMaster measurements, Dr. Dave Luce for giving us access to the Reichert ORA and Gary Gagarinas for assisting in laser refractive surgeries. Finally, our thanks to Dr. Jens Bühren for many constructive discussions and feedback on the manuscript.

Supported by National Eye Institute grant RO1 EY015836-01, a grant from Bausch & Lomb Inc. to the University of Rochester's Center for Visual Science, grants from the University of Rochester's Center for Electronic Imaging Systems, a NYSTAR-designated Center for Advanced Technology and by an unrestricted grant to the University of Rochester's Department of Ophthalmology from the Research to Prevent Blindness Foundation, Inc.

References

1. Moreno-Barriuso E, Lloves JM, Marcos S, Navarro R, Llorente L, Barbero S. Ocular aberrations before and after myopic corneal refractive surgery: LASIK-induced changes measured with laser ray tracing. Investigative ophthalmology and Visual Science 2001;42:1396 – 1403. [PubMed: 11328757]
2. Luce DA. Determining in vivo biomechanical properties of the cornea with an ocular response analyzer. Journal of Cataract and Refractive Surgery 2005;31:156 – 162. [PubMed: 15721708]
3. Roberts C. Biomechanics of the cornea and wavefront-guided laser refractive surgery. Journal of Refractive Surgery 2002;18:S589 – S592. [PubMed: 12361163]
4. Roberts, C.; Dupps, WJ. Corneal biomechanics and their role in corneal ablative procedures. In: MacRae, SM.; Krueger, RR.; Applegate, RA., editors. Customized Corneal Ablation The Quest For SuperVision. Thorofare: SLACK Incorporated; 2001. p. 109-131.
5. Yoon G, Cox I, MacRae SM. Spherical aberration induced by refractive surgery. ARVO. 2003
6. Fini ME. Keratocyte and fibroblast phenotypes in the repairing cornea. Progress in Retinal & Eye Research 1999;18:529 – 551. [PubMed: 10217482]
7. Jester JV, Petroll WM, Cavanagh HD. Corneal stromal wound healing in refractive surgery: the role of myofibroblasts. Progress in Retinal & Eye Research 1999;18:311 – 356. [PubMed: 10192516]
8. Telfair WB, Bekker C, Hoffman HJ, et al. Healing after photorefractive keratectomy in cat eyes with a scanning midinfrared Nd:YAG pumped optical parametric oscillator laser. Journal of Refractive Surgery 2000;16:32 – 39. [PubMed: 10693617]
9. Wilson SE. Analysis of the keratocyte apoptosis, keratocyte proliferation and myofibroblast transformation responses after photorefractive keratectomy and laser in situ keratomileusis. Transactions of the American Ophthalmological Society 2002;100:411 – 433. [PubMed: 12545703]
10. Wilson SE, Liu JJ, Mohan RR. Stromal-epithelial interactions in the cornea. Progress in Retinal & Eye Research 1999;18:293 – 309. [PubMed: 10192515]
11. Ramamirtham R, Norton TT, Siegwart JT, Roorda A. Wave aberrations of tree shrew eyes. Investigative Ophthalmology and Visual Science. 2003;(suppl)
12. Ramamirtham R, Roorda A, Kee C-S, Hung L-FF, Qiao Y, Smith EL. Wave aberrations in the young monkey eye. Investigative Ophthalmology and Visual Science. 2002;(suppl)
13. Coletta NJ, Toilo D, Moskowitz A, Nickla DL, Marcos S. Wavefront aberrations of the marmoset eye. Investigative Ophthalmology and Visual Science. 2003;(suppl)
14. Kisilak ML, Campbell MCW, Hunter JJ, Irving EL, Huang L. Monochromatic aberrations in the chick eye during emmetropization: goggled vs control eyes. Investigative Ophthalmology and Visual Science. 2003;(suppl)
15. Koh S, Maeda N, Kuroda T, et al. Effect of tear film break-up on higher-order aberrations measured with wavefront sensor. American Journal of Ophthalmology 2002;134:115 – 117. [PubMed: 12095817]
16. Huxlin KR, Pasternak T. Training-induced recovery of visual motion perception after extrastriate cortical damage in the adult cat. Cerebral Cortex 2004;14:81 – 90. [PubMed: 14654459]
17. Pasternak T, Maunsell JH. Spatiotemporal sensitivity following lesions of area 18 in the cat. Journal of Neuroscience 1992;12:4521–4529. [PubMed: 1432108]
18. Pasternak T, Tompkins J, Olson CR. The role of striate cortex in visual function of the cat. Journal of Neuroscience 1995;15:1940–1950. [PubMed: 7891143]
19. Pasternak T, Horn K. Spatial vision of the cat: variation with eccentricity. Visual Neuroscience 1991;6:151–158. [PubMed: 2049330]
20. Huxlin KR, Yoon G, Nagy L, Porter J, Williams DR. Monochromatic ocular wavefront aberrations in the awake-behaving cat. Vision Research 2004;44:2159 – 2169. [PubMed: 15183683]
21. Carrington SD, Woodward EG. Corneal Thickness and Diameter in the Domestic Cat. Ophthalmic & Physiological Optics 1986;6:385–389. [PubMed: 3627798]
22. Rufer F, Schroder A, Erb C. White-to-White Corneal Diameter Normal Values in Healthy Humans Obtained With the Orbscan II Topography System. Cornea 2005;24:259–261. [PubMed: 15778595]
23. Vakkur GJ, Bishop PO. The schematic eye in the cat. Vis Res 1963;3:375–381.
24. Hughes A. A supplement to the cat schematic eye. Vision Res 1976;16:149–154. [PubMed: 1266054]

25. Hughes, A. Handbook of Sensory Physiology, VII/5. Berlin: Springer Verlag; 1977. The topography of vision in mammals of contrasting life style: comparative optics and retinal organization.
26. Jester JV, Barry PA, Lind GJ, Petroll WM, Garana RMR, Cavanagh HD. Corneal keratocytes: in situ and in vitro organization of cytoskeletal contractile proteins. Investigative Ophthalmology and Visual Science 1994;35:730 – 743. [PubMed: 8113024]
27. Li HF, Petroll WM, Moller-Pedersen T, Maurer JK, Cavanagh HD, Jester JV. Epithelial and corneal thickness measurements by in vivo confocal microscopy through focusing (CMTF). Current Eye Research 1997;16:214 – 221. [PubMed: 9088737]
28. Hayashi S, Osawa T, Tohyama K. Comparative observations on corneas, with special reference to Bowman's layer and Descemet's membrane in mammals and amphibians. Journal of Morphology 2002;254:247 – 258. [PubMed: 12386895]
29. Meek KM, Boote C. The organization of collagen in the corneal stroma. Experimental Eye Research 2004;78:503 – 512. [PubMed: 15106929]
30. Boote C, Hayes S, Abahussin M, Meek KM. Mapping collagen organization in the human cornea: left and right eyes are structurally distinct. Investigative Ophthalmology and Vision Science 2006;47:901 – 908.
31. Jester JV, Petroll WM, Feng W, Essepian J, Cavanaugh HD. Radial keratotomy. 1. The wound healing process and measurement of incisional gape in two animal models using in vivo confocal microscopy. Investigative Ophthalmology and Visual Science 1992;33:3255 – 3270. [PubMed: 1428701]
32. Courville CB, Smolek MK, Klyce SD. Contribution of the ocular surface to visual optics. Experimental Eye Research 2004;78:417 – 425. [PubMed: 15106921]
33. Marcos S, Barbero S, Llorente L, Merayo-Lloves J. Optical response to LASIK surgery for myopia from total and corneal aberration measurements. Investigative Ophthalmology and Visual Science 2001;42:3349 – 3356. [PubMed: 11726644]
34. Llorente L, Barbero S, Merayo J, Marcos S. Total and corneal optical aberrations induced by laser in situ keratomileusis for hyperopia. Journal of Refractive Surgery 2004;20:203 – 216. [PubMed: 15188896]
35. Petroll WM, Cavanagh HD, Jester JV. Assessment of stress fiber orientation during healing of radial keratotomy wounds using confocal microscopy. Scanning 1998;20:74 – 82. [PubMed: 9530870]
36. Telfair WB, Bekker C, Hoffman HJ, et al. Histological comparison of corneal ablation with ER:YAG laser, Nd:YAG optical parametric oscillator, and excimer laser. Journal of Refractive Surgery 2000;16:40 – 50. [PubMed: 10693618]
37. Thibos, LN.; Applegate, RA.; Schwiegerling, JT.; Webb, RV.; Members, VST. Standards for reporting the optical aberrations of eyes. In: MacRae, SM.; Kruger, RR.; Applegate, RA., editors. Customized Corneal Ablation The Quest For SuperVision. Thorofare: SLACK Incorporated; 2001. p. 348-361.
38. Radhakrishnan S, Rollins AM, Roth JE, et al. Real-time optical coherence tomography of the anterior segment at 1310 nm. Archives of Ophthalmology 2001;119:1179 – 1185. [PubMed: 11483086]
39. Wang J, Thomas J, Cox I, Rollins A. Noncontact measurements of central corneal epithelial and flap thickness after laser in situ keratomileusis. Investigative Ophthalmology and Visual Science 2004;45:1812 – 1816. [PubMed: 15161844]
40. Luce DA. Methodology for Cornea Compensated IOP and Corneal Resistance Factor for the Reichert Ocular Response Analyzer. ARVO. 2006
41. Reinstein DZ, Silverman RH, Rondeau MJ, Coleman DJ. Epithelial and corneal thickness measurements by high-frequency ultrasound digital signal processing. Ophthalmology 1994;101:140 – 146. [PubMed: 8302547]
42. Phillips LJ, Cakanac CJ, Eger MW, Lilly ME. Central corneal thickness and measured IOP: a clinical study. Optometry 2003;74:218–225. [PubMed: 12703686]
43. Phillips LJ, Cakanac CJ, Eger MW, Lilly ME. Central corneal thickness and measured IOP: a clinical study. Optometry 2003;74:218 – 225. [PubMed: 12703686]
44. Barkana Y, Gerber Y, Elbaz U, et al. Central corneal thickness measurements with the Pentacam Scheimpflug system, optical low-coherence reflectometry pachymeter, and ultrasound pachymetry. Journal of Cataract and Refractive Surgery 2005;31:1729 – 1735. [PubMed: 16246776]

45. Lackner B, Schmidinger G, Pieh S, Funovics MA, Skorpik C. Repeatability and reproducibility of central corneal thickness measurements with Pentacam, Orbscan and ultrasound. Optometry and Vision Science 2005;82:892 – 899. [PubMed: 16276321]
46. Sheng H, Bottjer CA, Bullimore MA. Ocular component measurement using the Zeiss IOLMaster. Optometry and Vision Science 2004;81:27 – 34. [PubMed: 14747758]
47. Hjortdal JO, Moller-Pedersen T, Ivarsen A, Ehlers N. Corneal power, thickness, and stiffness: results of a prospective randomized controlled trial of PRK and LASIK for myopia. Journal of Cataract and Refractive Surgery 2005;31:21 – 29. [PubMed: 15721693]
48. Comaish IF, Lawless MA. Progressive post-LASIK keratectasia. Biomechanical instability or chronic disease process? Journal of Cataract and Refractive Surgery 2002;28:2206 – 2213. [PubMed: 12498861]
49. Guirao A. Theoretical elastic response of the cornea to refractive surgery: risk factors for keratectasia. Journal of Refractive Surgery 2005;21:176 – 185. [PubMed: 15796224]
50. Dupps WJ. Biomechanical modeling of corneal ectasia. Journal of Refractive Surgery 2005;21:186 – 190. [PubMed: 15796225]
51. Maurice, DM. The cornea and sclera. In: Davson, H., editor. The Eye. Orlando, Fl: Academinc Press; 1984.
52. Boote C, Dennis S, Meek KM. Spatial mapping of collagen fibril organization in primate cornea - an X-ray diffraction investigation. Journal of Structural Biology 2004;146:359 – 367. [PubMed: 15099577]
53. Muller LJ, Pelzs E, Schurmans LRHM, Vrensen GFJM. A new three-dimensional model of the organization of proteoglycans and collagen fibrils in the human cornea. Experimental Eye Research 2004;78:493 – 501. [PubMed: 15106928]
54. Dupps WJ, Wilson SE. Biomechanics and wound healing in the cornea. Experimental Eye Research 2006:1–12.
55. Acosta AC, Espana EM, Stoiber J, et al. Corneal stroma regeneration in felines after supradescemetic keratoprosthesis implantation. Cornea 2006;25:830 – 838. [PubMed: 17068461]
56. Moller-Pedersen T, Li HF, Petroll WM, Cavanagh HD, Jester JV. Confocal microscopic characterization of wound repair after photorefractive keratectomy. Investigative Ophthalmology and Visual Science 1998;39:487 – 501. [PubMed: 9501858]
57. Moller-Pedersen T, Cavanagh HD, Petroll WM, Jester JV. Stromal wound healing explains refractive instability and haze development after photorefractive keratectomy. A 1-year confocal microscopic study. Ophthalmology 2000;107:1235 – 1245. [PubMed: 10889092]
58. Moller-Pedersen T, Cavanagh HD, Petroll WM, Jester JV. Neutralizing antibody to TGFbeta modulates stromal fibrosis but not regression of photoablative effect following PRK. Current Eye Research 1998;17:736 – 747. [PubMed: 9678420]
59. Fantes FE, Hanna KD, Waring GO, Pouliquen Y, Thompson KP, Savoldelli M. Wound healing after excimer laser keratomileusis (photorefractive keratectomy) in monkeys. Archives of Ophthalmology 1990;108:665 – 675. [PubMed: 2334323]
60. Dawson DG, Edelhauser HF, Grossniklaus HE. Long-terms histopathologic findings in human corneal wounds after refractive surgical procedures. American Journal of Ophthalmology 2005;139:168 – 178. [PubMed: 15652843]
61. Amano S, Shimizu K, Tsubota K. Corneal epithelial changes after excimer laser photorefractive keratectomy. American Journal of Ophthalmology 1993;115:441 – 443. [PubMed: 8470714]
62. Lohmann CP, Patmore A, O'Brart D, Resischl U, Winkler Mohrenfels C, Marshall J. Regression and wound healing after excimer laser PRK: a histopathological study on human corneas. European Journal of Ophthalmology 1997;7:130 – 138. [PubMed: 9243215]
63. Seiler T, Kaemmerer M, Mierdel P, Krinke H-E. Ocular optical aberrations after photorefractive keratectomy for myopia and myopic astigmatism. Archives of Ophthalmology 2000;118:17 – 21. [PubMed: 10636408]
64. Mierdel P, Kaemmerer M, Krinke H-E, Seiler T. Effects of photorefractive keratectomy and cataract surgery on ocular optical errors of high order. Graefes' Archives of Clinical and Experimental Ophthalmology 1999;237:725 – 729.

65. Porter J, Yoon G, Lozano D, et al. Aberrations induced in wavefront-guided laser refractive surgery due to shifts between natural and dilated pupil centers. Journal of Cataract and Refractive Surgery 2006;32:21–32. [PubMed: 16516775]

66. Mrochen M, Kaemmerer M, Mierdel P, Seiler T. Increased higher-order optical aberrations after laser refractive surgery: a problem of subclinical decentration. Journal of Cataract and Refractive Surgery 2001;27:362 – 369. [PubMed: 11255046]

67. O'Brart DPS, Gartry DS, Lohmann CP, Muir MGK, Marshall J. Excimer laser photorefractive keratectomy for myopia: comparison of 4.00- and 5.00-millimeter ablation zones. Journal of Refractive & Corneal Surgery 1994;10:87 – 94. [PubMed: 7517293]

68. O'Brart DPS, Corbett MC, Lohmann CP, Kerr Muir MG, Marshall J. The effects of ablation diameter on the outcome of excimer laser photorefractive keratectomy. Arch Ophthalmol 1995;113:438–443. [PubMed: 7710392]

69. Mok K, Lee V. Effect of optical zone ablation diameter on LASIK-induced higher order optical aberrations. J Refract Surg 2005;21:141–143. [PubMed: 15796217]

70. Bühren J, Kühne C, Kohnen T. Influence of pupil and optical zone diameter on higher order aberrations after wavefront-guided myopic LASIK. Journal of Cataract and Refractive Surgery 2005;31:2272 – 2280. [PubMed: 16473217]

71. Endl MJ, Martinez CE, Klyce SD, et al. Effect of larger ablation zone and transition zone on corneal optical aberrations after photorefractive keratectomy. Archives of Ophthalmology 2001;119:1159 – 1164. [PubMed: 11483083]

72. Seo KY, Lee JB, Kang JJ, Lee ES, Kim EK. Comparison of higher-order aberrations after LASEK with a 6.0mm ablation zone and a 6.5mm ablation zone with blend zone. J Cataract Refract Surg 2004;30:653–657. [PubMed: 15050263]

73. O'Brart DPS, Patsoura E, Jaycock P, Rajan M, Marshall J. Excimer laser photorefractive keratectomy for hyperopia: 7.5 year follow-up. Journal of Cataract and Refractive Surgery 2005;31:1104 – 1113. [PubMed: 16039483]

74. Rajan MS, HJaycock P, O'Brart DPS, Nystrom HH, Marshall J. A long-term study of photorefractive keratectomy: 12 year follow-up. Ophthalmology 2004;111:1813 – 1824. [PubMed: 15465541]

Biography

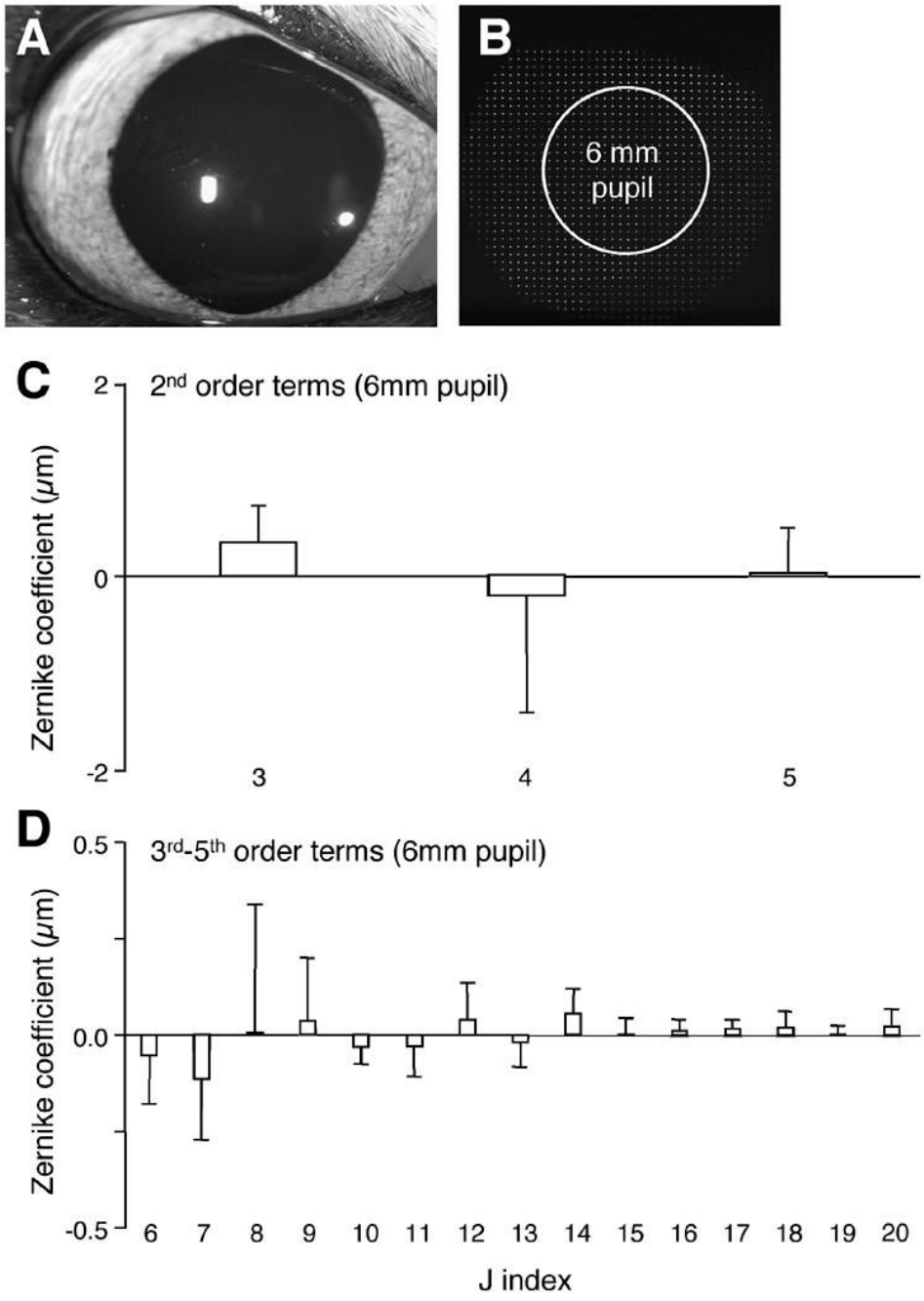

Figure 1.

Wavefront aberrations in the normal cat eye. **A**. Photograph of a pre-operative feline eye and a sample feline spot array pattern (**B**) collected in the awake-behaving state using our modified Shack-Hartmann wavefront sensor. Note the shadow created over the spot array pattern by the upper eyelid is well beyond the 6mm analysis pupil used to measure wave aberrations. **C**. Pre-operative, lower-order wave aberrations for the 10 cats that underwent PRK as part of the present study. Note the small magnitude of lower order aberrations, including defocus (j=4) and the two astigmatism terms (j=3 and 5). **D**. Pre-operative Zernike coefficient values for higher order aberrations (up to 5^{th} order Zernike coefficients, j=20) were also relatively low.

In particular, note the small amount of spherical aberration (j=12) in our sample of cat eyes. Values are expressed as means ± SD.

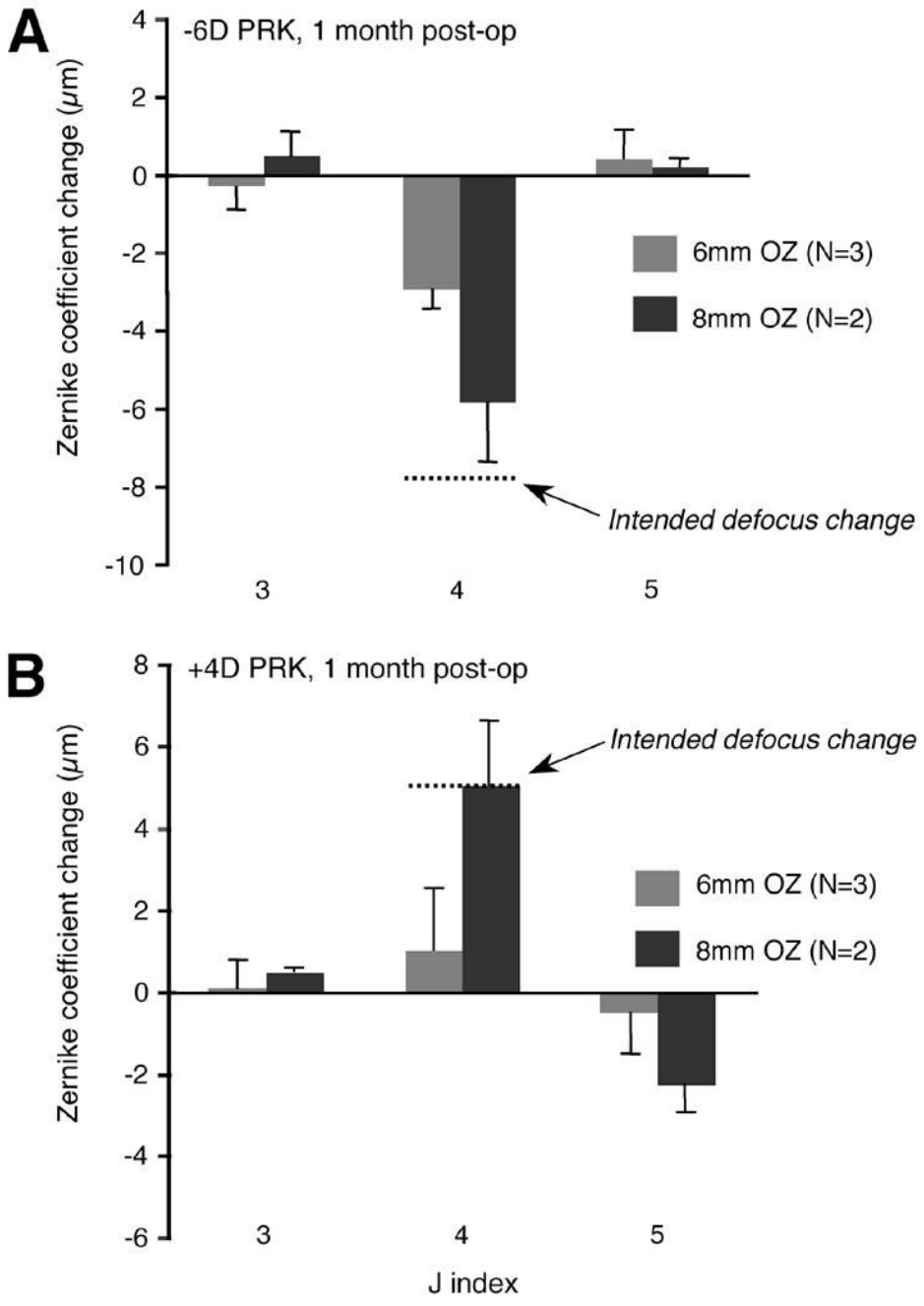

Figure 2.

Change in the magnitude of lower order wavefront aberrations (j indices 3 to 5) between pre-operative values and values at 1 month after myopic (**A**) and hyperopic (**B**) PRK in the cat. Note the significantly lower magnitude of defocus change (j=4) achieved by ablations over 6 versus 8mm optical zones (OZs). Defocus values for 6mm OZs were well below the intended defocus change (dotted line). No significant differences were observed for the amount of astigmatism change induced by either type of surgery. Values are expressed as means ± SD. N= number of eyes treated in each group.

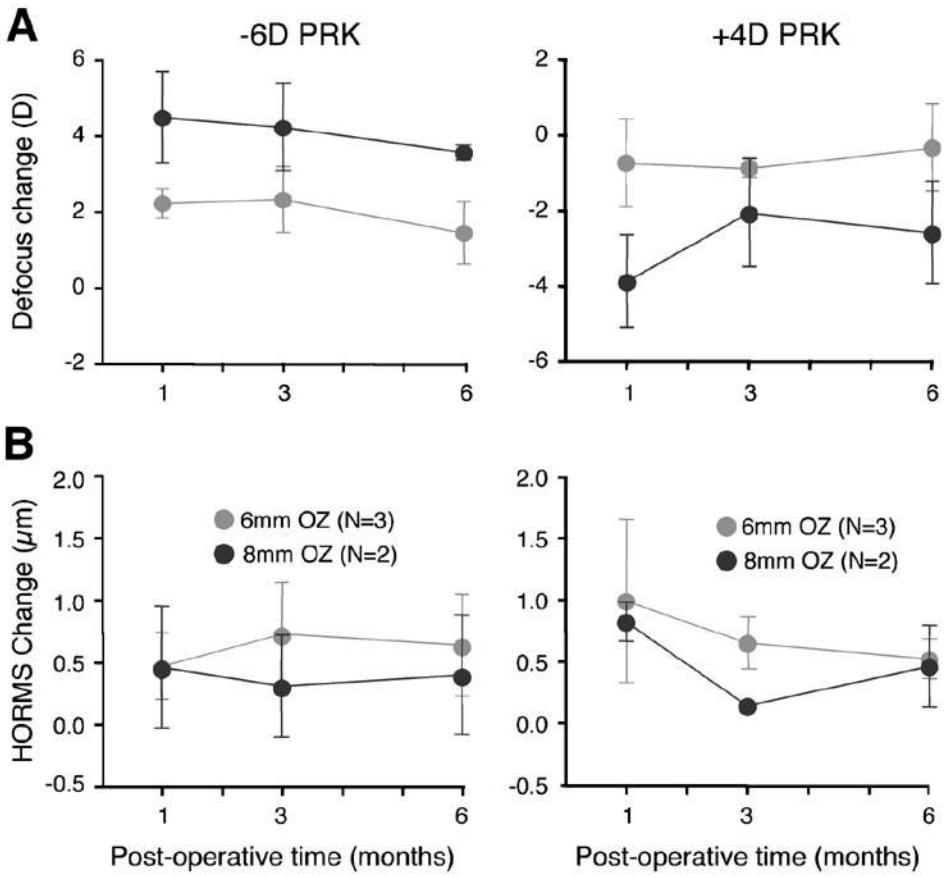

Figure 3.

Change in the magnitude of higher order wavefront aberrations (j indices 6 to 20) between pre-operative values and values at 1 month after myopic (**A**) and hyperopic (**B**) PRK in the cat. No systematic differences were observed between changes induced over 6 or 8mm optical zones (OZs) following either -6D myopic or +4D hyperopic PRK. Spherical aberration (j=12) increased in the positive direction after myopic PRK and in the negative direction after hyperopic PRK, regardless of OZ size. The magnitude of vertical and horizontal coma terms (j=7 and 8 respectively) increased, but this was not consistently related to the optical zone size. Values are expressed as means ± SD. N = number of eyes treated in each group.

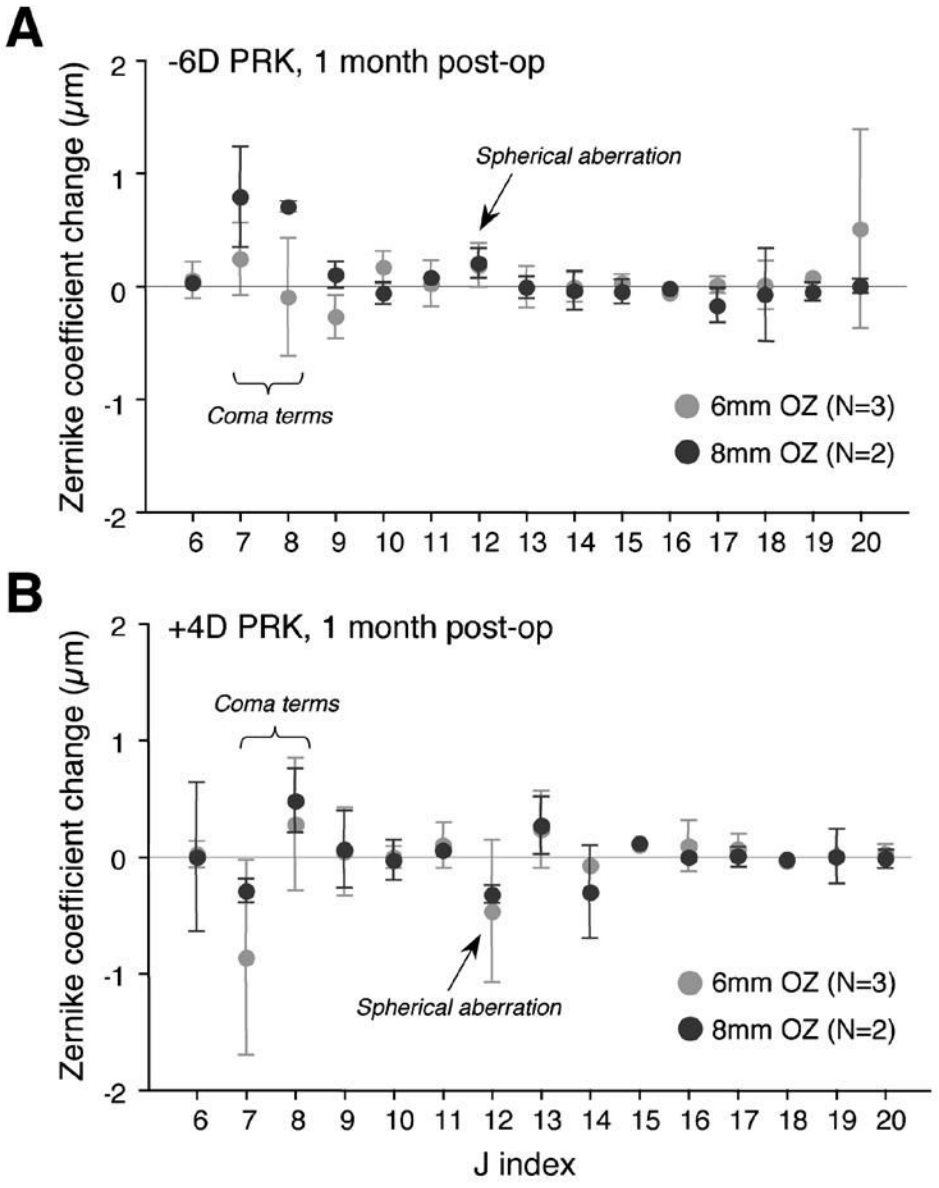

Figure 4.

Stability of refractive changes induced over a 6 months period by PRK over 6 or 8mm OZs in the cat. **A**. No significant differences were observed between 1 and 6 months for any of the experimental groups with respect to dioptric change in the defocus term from pre-operative values for either 6D myopic or 4D hyperopic PRKs. **B**. Higher order RMS change from pre-operative values also showed no significant regression between 1 and 6 months post-PRK. Values are expressed as means ± SD. N = number of eyes treated in each group.

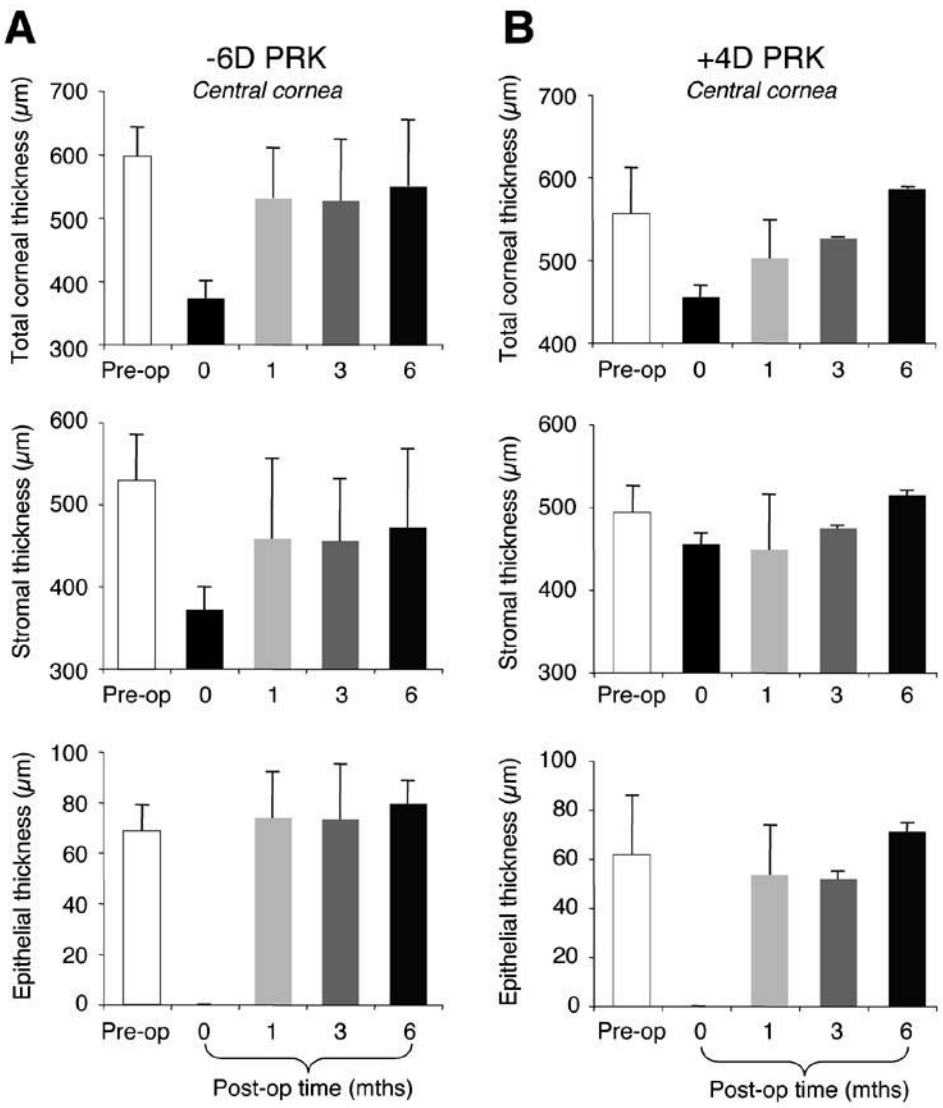

Figure 5.

Effects of PRK on central thicknesses of the cat cornea, as measured using OCT. **A**. Plots of mean central thickness of the total cornea, the stromal layer and the epithelial layer in cats that underwent myopic PRK over 8mm OZs (N=2). Total central corneal thickness decreased by ~200μm following PRK, but returned to normal by 1 month post-operatively. Most of this increase appeared driven by stromal remodeling. Epithelial thickness decreased to 0μm as a result of PRK, but returned to normal by 1 month post-operatively, remaining at that level over the next 5 months. **B**. Plots of mean central thickness of the total cornea, the stromal layer and the epithelial layer in cats that underwent hyperopic PRK over 8mm OZs (N=2). Total central corneal thickness decreased by only ~100μm following PRK, and gradually returned to normal over the next 6 months. Unlike cats with myopic PRK, the remodeling of central corneal thickness in cats with hyperopic PRK appeared driven fairly equally by stromal and epithelial regrowth. Values are expressed as means ± SD.

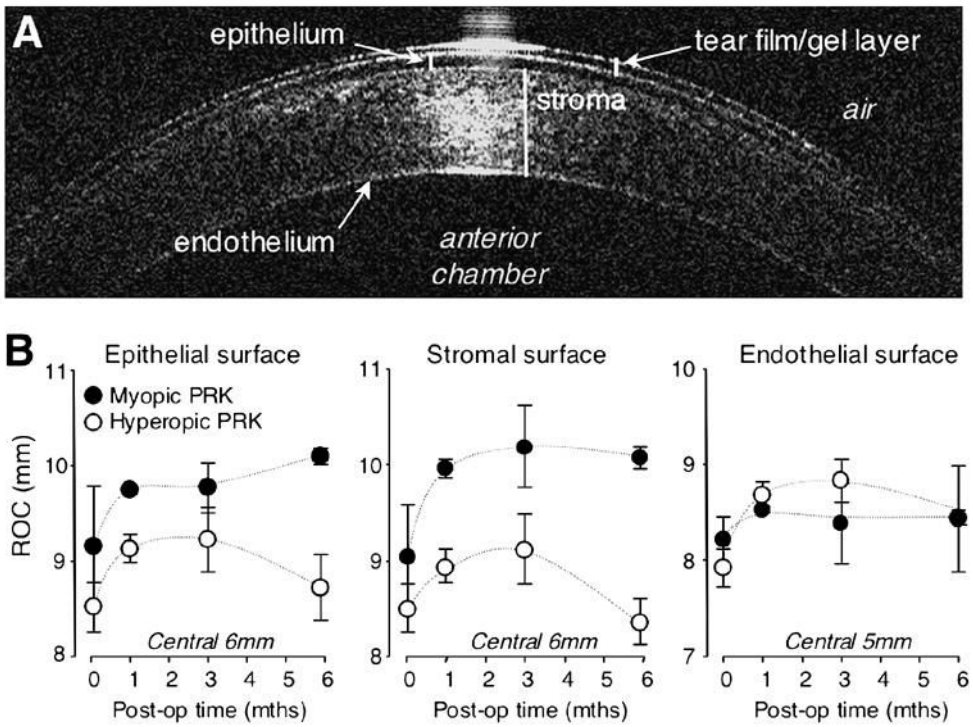

Figure 6.

Effects of PRK on central radii of curvature of the cat cornea, as measured using OCT. **A**. Sample OCT image of the cat cornea, illustrating the different visible layers (protective gel layer, epithelium, stroma and endothelium), as well as the relative location of the air and anterior chamber of the eye. **B**. Plots of mean radii of curvature of the epithelial, stromal and endothelial surfaces of the cat cornea pre-operatively, as well as 1, 3 and 6 months after PRKs over 8mm OZs. Data for cats that underwent myopic PRK are represented by dark grey symbols while data for cats that underwent hyperopic PRK are indicated by white symbols. Note that all animals exhibited an increase in radius of curvature over the central 6mm of cornea following surgery, although hyperopic PRK caused less of a flattening than myopic PRK and this flattening became a steepening by 6 months post-surgery, particularly at the epithelial and stromal surfaces. By contrast, cats with myopic PRKs exhibited a strong increase in corneal radius of curvature at 1 month after surgery, and maintained this flattening throughout the post-operative period examined. Note also all three corneal surfaces exhibited some amount of flattening, including the endothelial surface, although this was not statistically significant for the latter. Values are expressed as means ± SD.

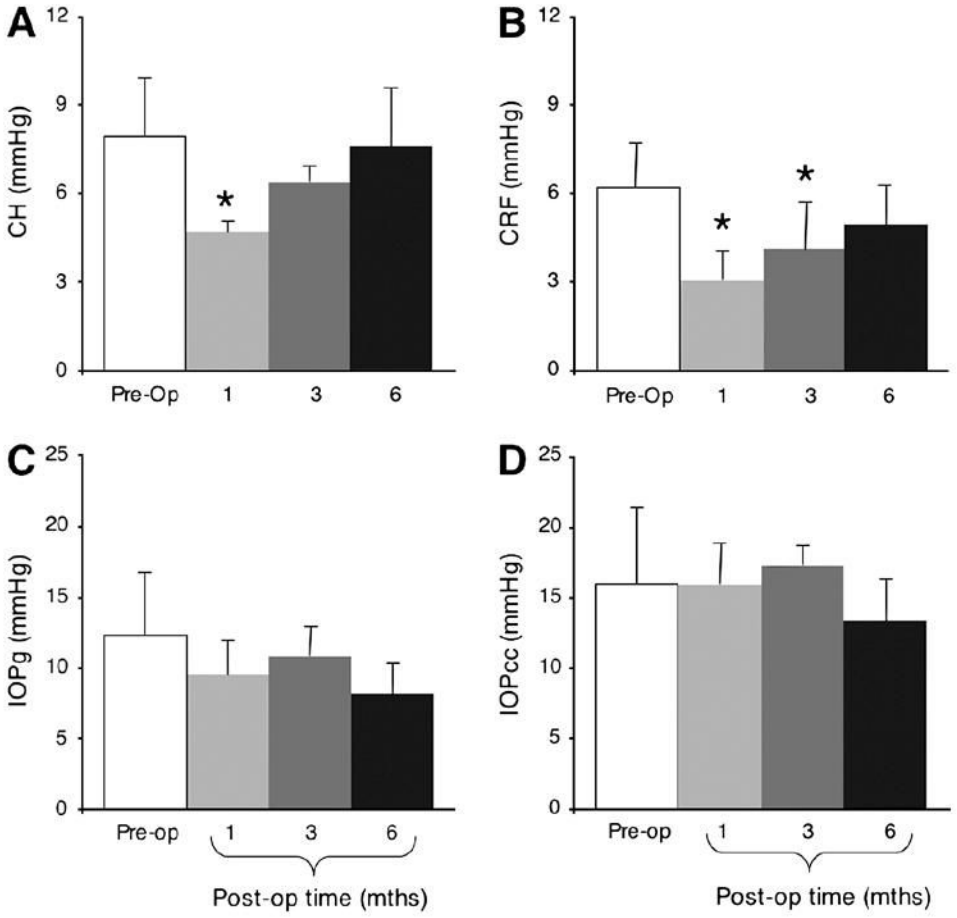

Figure 7.

Effects of PRK on visco-elastic properties of the cat cornea and on intraocular pressure. Cats from all surgical groups (myopic and hyperopic PRK, over 6 and 8mm OZs) were combined for this analysis. **A**. Ablated corneas exhibited a significant decrease in corneal hysteresis (CH) 1month after PRK relative to pre-operative values, but they recovered towards normal values at 3 and 6 months post-operatively. **B**. The Corneal Resistance Factor (CRF) was lowest 1month post-PRK, recovering slowly over the next 5 months so that by 6 months post-operatively, it was not significantly different from pre-operative values. **C.** Corresponding histogram for Goldmann-like intraocular pressure measurements (IOPg) shows that PRK does not significantly change IOPg in cats. **D**. Similarly, cornea-compensated intraocular pressure (IOPcc) remained unchanged following PRK. Values are expressed as means ± SD. * = significant difference from pre-operative values at $P<0.05$ level, two-tailed Student's t-test.

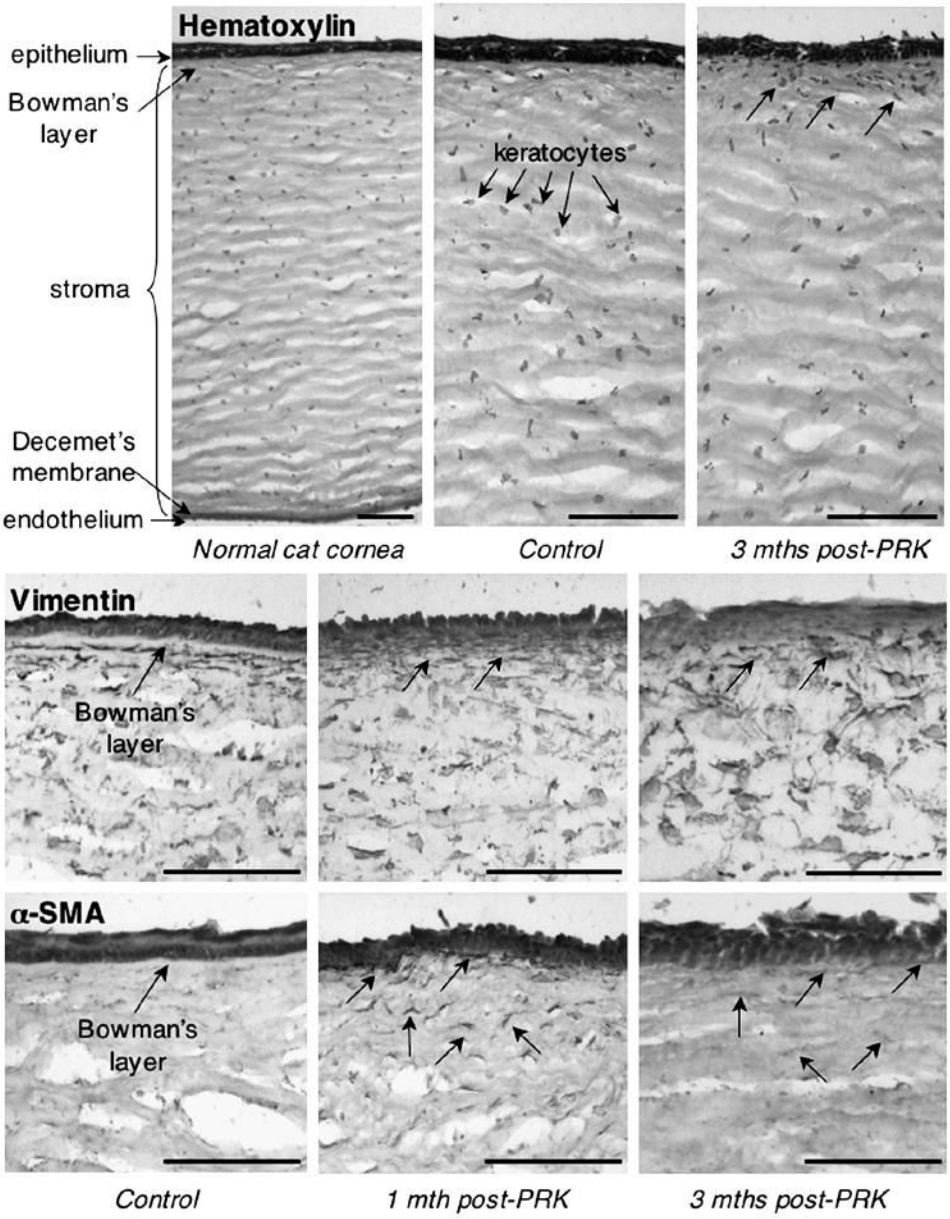

Figure 8.

Histopathology of the cat cornea after PRK. Hematoxylin staining of the normal cat cornea shows histological structure consistent with that previously published and including a stratified epithelium, Bowman's layer, a stroma populated by keratocytes, a very thin Decemet's membrane and an endothelium. Note that 3 months after PRK, the cat cornea exhibited a typical cellular response, with an increased density of stromal keratocytes immediately under the ablation epithelium (arrowed). Vimentin immuno-labeling showed a population of quiescent keratocytes in the normal cat stroma, which increases in density at 1 and 3 months after PRK. Note the absence of a clearly demarcated Bowman's layer after PRK. αSMA immuno-staining shows lack of stromal reactivity before PRK, but increased expression in stromal keratocytes (myofibroblasts - arrowed) under the ablation 1 month after PRK. This reactivity decreased by 3 months post-PRK, although some faintly-labeled cells could still be seen in the sub-ablation stroma (arrowed). Scale bars = 100μm.

Table 1

Comparison of native cat and human ocular biometrics.

Parameter	Mean ± SD	
	Cat	Human
Corneal thickness (μm)	575 ± 53	552 ± 32[†]
Epithelial thickness (μm)	54.0 ± 20.3	50.6 ± 3.9[†]
IOPg (mm Hg)[*]	12.3 ± 4.5	15.7 ± 2.9
IOPcc (mm Hg)	16.0 ± 5.4	14.8 ± 3.7
Corneal hysteresis (mm Hg)[*]	7.9 ± 2.0	11.1 ± 0.8
Corneal resistance factor (mm Hg)[*]	6.2 ± 1.5	10.0 ± 0.9

[*] Significant difference between cat and human values ($P \leq .05$, Student *t* test)

[†] Values for human subjects not measured in the present study but obtained from Li HF, Petroll WM, Møller-Pedersen T, et al. Epithelial and corneal thickness measurements by in vivo confocal microscopy through focusing (CMTF). Curr Eye Res 1997; 16:214–221

IOPcc = cornea-compensated IOP; IOPg = Goldmann-like IOP